Title	Molecular Dynamics Study of Interactions between the Water/ice Interface and a Nanoparticle in the Vicinity of a Solid Surface
Author(s)	Uchida, Shota; Fujiwara, Kunio; Shibahara, Masahiko
Citation	Nanoscale and Microscale Thermophysical Engineering. 2020, 24(2), p. 53-65
Version Type	AO
URL	https://hdl.handle.net/11094/93594
rights	© 2020 Taylor & Francis.
Note	

Molecular Dynamics Study of Interactions between the Water/ice Interface and a Nanoparticle in the Vicinity of a Solid Surface

Shota Uchida[1,2,*], Kunio Fujiwara[1], Masahiko Shibahara[1]

[1] *Graduate School of Engineering, Osaka University, 2-1 Yamadaoka, Suita, Osaka 565-0871, Japan*

[2] *SCREEN Holdings Co., Ltd., 322 Furukawa-cho, Hazukashi, Fushimi-ku, Kyoto, Kyoto 612-8486, Japan*

[*] sh.uchida@screen.co.jp

Molecular Dynamics Study of Interactions between the Water/ice Interface and a Nanoparticle in the Vicinity of a Solid Surface

In this study, non-equilibrium molecular dynamics simulations were conducted for a coexistence system of water and ice on a wall surface with a single nanoparticle to reveal the effects of water solidification on the nanoparticle in the vicinity of a wall surface. We further investigated the effect of the presence and size of particles on the density profile of water in the vicinity of the wall surface and the force acting on particles from water molecules, when the solidification interface contacted the wall and the particles. The results revealed that a strong mutual influence exists between the solidification interface and the nanoparticle on the wall's surface; the nanoparticle on the wall prevents water solidification in proximity to the wall. Moreover, the force acting on the nanoparticle from water molecules changes as the solidification interface approaches; the cooling temperature is shown to affect the direction of this force. It indicates that the solidification process is a key influential factor which affects nanoparticle movements on a wall surface at molecular scales.

Keywords: Non-equilibrium molecular dynamics, Solidification, Ice/water interface, Nanoparticle

Introduction

In the semiconductor manufacturing process, it is essential to remove nanoparticles that cause defects in the semiconductor device during wet cleaning without damaging the semiconductor pattern [1]. However, the conventional cleaning method makes the removal of the nanoparticles without damaging the pattern difficult, because of the semiconductor miniaturization. As one solution for this problem, a new cleaning method using a solidification process has been proposed [2, 3]. During this cleaning process, a liquid film on the wafer is frozen by cold nitrogen gas, and the nanoparticles are removed with a cleaning liquid. The experimental results showed that this process reduces damage to the semiconductor pattern and increases the particle removal rate, which implies that the solidification phenomenon can affect the nanoparticles at the nanoscale [3]. However, the mechanism of this phenomenon is unclear because of the difficulty of observation due to the level of semiconductor miniaturization lower than dozens of nanometers. In order to improve the particle removal rate on the semiconductor wafer, it is necessary to fully understand the mechanism of the particle removal processes in the solidification cleaning process.

Experimental studies have explained several features concerning the structural and dynamic properties of liquid and solid systems at nanoscales; these include X-ray [4, 5] and NMR [6, 7, 8] observations on the dynamics and phase change phenomena of water in a nanometer scale pore. The interactions between particles and the solidification interface have been investigated both experimentally and theoretically. At the micrometer scale, numerous theories about the ice–water solidification surface advancing “critical velocity”, below which the particles are rejected by the interface, and above which they are trapped in the ice have been proposed [9], and the experimental results have been shown to be consistent with the theories [10]. On the other hand, at the nanometer scale, experimental studies have been conducted to observe the nature of the interactions (e.g., pushing, rolling, sliding) of gold nanoparticles on ice solidification interface by TEM [11]. However, few studies to date have captured the movement of nanoparticles at nanoscales and the mechanism of nanoparticle movement by the solidification interface is still unclear.

Conversely, molecular dynamics simulations contribute to the understanding and interpretation of nanoscale phenomena. There are some previous studies concerning the dynamics of water molecules near the ice–water solidification interface. For example, the dynamics of water molecules at the solidification interface depends on the plane orientation of the ice [12]. Also, the difference in hydrogen bond formation mechanism at the solidification interface is related to the difference in crystal growth rate for each plane orientation [13]. Previous studies focusing on the dynamics of molecules in proximity to a wall have reported that the density profile [14], diffusivity [15] and hydrogen bonding [16] of molecules are different from the bulk due to the influence of the wall. Moreover, it has been shown that wall vibrations [17], plane orientation and electric field [18] affect the properties of water molecules and ice crystal nucleation in the vicinity of the wall surface. Previous studies on the growth of the solidification interface on the wall show that the interaction strength between water molecules and the wall affects the solidification phenomena near the wall [19].

However, no studies have addressed the issue of particle removal on semiconductor wafers, and little is known about the interaction between particle removal and the solidification interface.

The purpose of this study is to clarify solidification interface effects on a particle on a wall's surface. Non-equilibrium molecular dynamics simulations were performed using an ice–water coexistence system, which comprised a TIP4P/2005 water model, and nanoparticles of a silicon (Si) atom on a wall surface with an FCC structure. Below the melting point in the system, the solidification interface grew toward the nanoparticle and the forces from the solidification interface acting on the nanoparticle were examined in detail. This study assessed the density distribution of water molecules in the vicinity of the wall and the interaction between the nanoparticle displacement and the force exerted by the water molecules.

This manuscript is organized as follows. Section 2 provides details of the simulation procedure, and Section 3 discusses the main results. Section 4 summarizes this study's conclusions.

Computational Methods

Calculation Conditions

This study performed molecular dynamics simulations using a system composed of an ice–water coexistence system with two types of particle on a wall surface, as shown in Fig. 1 (a). The ice–water coexistence system contained 1224 (3672 atoms) water molecules, and the wall was composed of 199 Pt atoms with an FCC structure. One particle was composed of 32 Si atoms (Particle 1) and the other was 16 atoms (Particle 2) and have a diameter of 1.0 nm (Particle 1) and 0.7 nm (Particle 2). The size of the calculation system was $L_x \times L_y \times L_z$ = 2.20 nm × 2.33 nm × 10.0 nm. The x and y directions had periodic boundary conditions and a mirror surface boundary condition was applied to the upper side of the z direction. A vacuum region of about 1.0 nm in the z direction was set above the ice region as the initial condition and the z direction origin is the wall surface. The ice region was of a Ih structure and the plane orientation of the ice water interface was $\{11\bar{2}0\}$. The wall consisted of Pt with a FCC structure and the plane orientation of the wall surface was $\{100\}$. The lattice constant of the wall structure was adjusted to be equal to that of the ice crystal lattice. The wall was composed of four layers with a fixed layer at the bottom of the wall. The Langevin method [20] of temperature control was applied, with the layer above the fixed layer acting as a phantom layer.

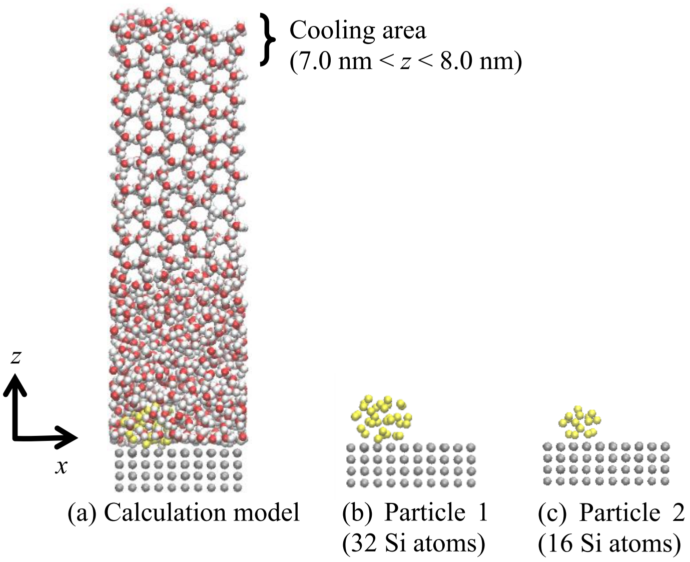

Figure 1. Calculation model and particles used in this study.

In this study, the TIP 4 P/2005 [21] model was adopted for the water molecule, and the Stillinger–Weber (SW) potential [22] was used for the calculation between the Si atoms that constituted the particles. The interactions between Pt–Pt atoms, which constituted the wall surface, and the interactions between different atoms were calculated by using the 12-6 Lennard-Jones (LJ) potential.

$$\phi_{ij}(r_{ij}) = 4\varepsilon_{ij}\left\{\left(\frac{\sigma_{ij}}{r_{ij}}\right)^{12} - \left(\frac{\sigma_{ij}}{r_{ij}}\right)^{6}\right\} \tag{1}$$

where *i* and *j* are the numbers of the atom and r_{ij} is the distance between the two atoms. The Lorenz–Berthelot mixing rule was used to obtain the σ_{ij} and ε_{ij} between different atoms. Table 1 contains the parameters used for calculating the LJ system. The velocity Berlet method was used for the numerical integration. The time step width was 2.0 fs for the LJ system and 0.1 fs for the SW system, and the RESPA algorithm method was used. The LAMMPS [23] software package was used for calculations.

Table 1. Interaction parameters of the 12-6 Lennard–Jones potential function.

	σ Å	ε kcal/mol
O–Pt	2.96	1.70
O–Si	2.62	3.04
Pt–Si	2.43	28.03
Pt–Pt	2.77	15.71

Simulation Procedure

Prior to calculating with the system shown in Fig. 1, the melting point of the water–ice wall system without particles was confirmed. A model was prepared that was equivalent in size to that in Fig. 1 and which did not contain particles. Then, the target temperatures (of 240, 244, 245, and 246 K) were used to investigate the melting point in accordance with the following procedure. First, the Nosé–Hoover method was used to heat the entire system from 1 K to the target temperature for 1 ns. Second, calculations were performed for a duration of 5ns, and the results were obtained. The temperature of the wall phantom layer was equivalent to the system control temperature in the Langevin method.

Figure 2 shows the time dependence of water molecule temperature and total energy (i.e., the sum of kinetic and potential energy) at each controlled temperature. When water molecules are controlled at the target temperature, the total energy declines due to ice crystallization under low temperature conditions, which indicates that the potential energy of water molecules decreases due to crystallization [24, 25]. Conversely, the total energy increases and ice melts under conditions of high temperature. Therefore, the melting point in this calculation system can be assumed to be 245 K, as the total energy remains almost constant with time at this temperature.

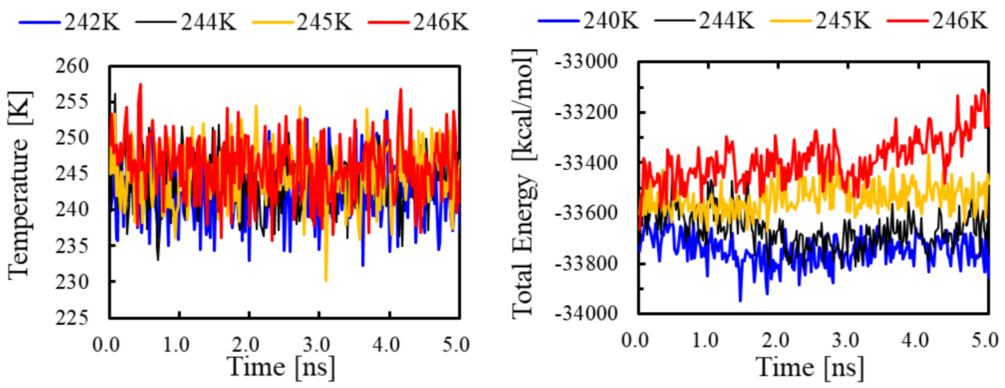

(a) Water temperature (b) Total energy of water molecules

Figure 2. Time evolution of temperature and total energy in the calculation system.

The following section describes the introduction of a particle and the calculation procedure. By applying the calculation system presented in Fig.1, the water molecules near the wall are eliminated in order to place a particle. The numerical procedure is as follow. After increasing the temperature of the entire system from 1 K to 242 K in 1 ns; we calculated without temperature control in 1ns for relaxation. Subsequently, the temperature of the water molecules at the cooling area (the region above the solid phase: 7.0 nm < *z* < 8.0 nm as illustrated in Fig. 1 (a)), named the cooling temperature in this study, was controlled using the velocity scaling method. During the entire calculation period, the wall temperature was maintained at 242 K to prevent the unintentional melting of the ice phase and to accelerate the start of ice crystallization.

Results and Discussion

The following section first discusses the influence of the presence and size of particles on the growth of ice crystals near the wall. It then describes particle displacement and the forces acting when the solidification interface approaches the particles. Finally, the effect of cooling temperature on the forces acting on the particles is discussed.

Density Distribution in the Vicinity of the Wall

This study calculated the instances without particles, with Particle 1, and with Particle 2 in Figure 1 at the cooling temperature of 240 K. Figure 3 shows the snapshots of Particle 1 at each time interval of the model and Fig. 4 illustrates the density profile of water molecules in the cases with and without particles. In Fig. 3, ice solidification grows toward the wall surface, and the particles move horizontally on the wall regardless of the solidification interface. The density profiles were calculated as the time averaged values between 25 ns and 50 ns and were computed for each condition by averaging the histogram of densities along z over the set of 1000 configurations. The width of the density histogram was 0.01nm. The time averaging span was determined by snapshots that reveal the solidification interface grows in proximity to the particle.

In the region near the wall (0.0 nm $< z <$0.5 nm) of the density profile (Fig. 4), an adsorption layer of water is formed on the wall. Conversely, the area at $z > 0.5$ nm from the wall demonstrates periodic peak values in density distribution. This is because water molecules are structured in the form of ice crystals, and the larger the intensity of the density peak, the more ice crystals are formed over a longer duration.

In the snapshot of $t = 40$ ns in Fig. 3, the solidification interface does not reach the wall and a liquid area remains. An ice crystal state is not maintained on the wall and the water state fluctuates between liquid and solid (ice), which implies that ice crystals are hardly formed in the region of 0.0 nm $< z <$0.5 nm. This area between the wall and the solidification interface is known as a quasi-liquid layer as observed by X-ray reflectivity profiles [26].

Next, we focus on the z coordinate position of the density peak in the range of 0.8 nm $< z <$1.0 nm. The z position of the density peak is close to the wall in the case without a particle, and the z-position of the density peak moves farther from the wall as the particle size increases, indicating that the formation of ice crystals is affected by the particle. It is evident that a correlation exists between particle size and the distance from the ice interface to the wall's surface.

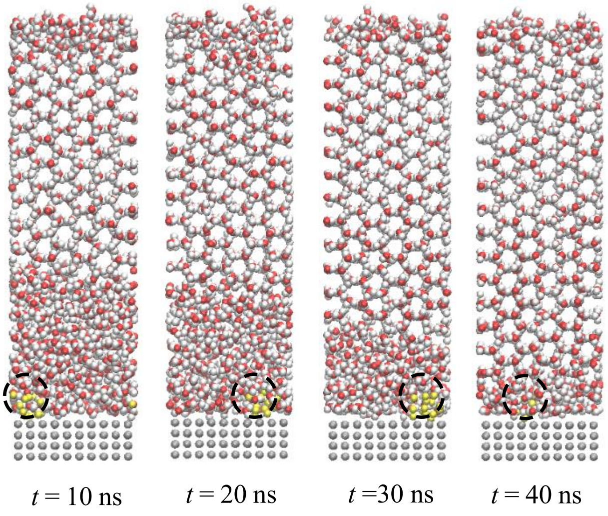

Figure 3. Snapshots in the solidification process in the case of *T* = 240 K with Particle 1.

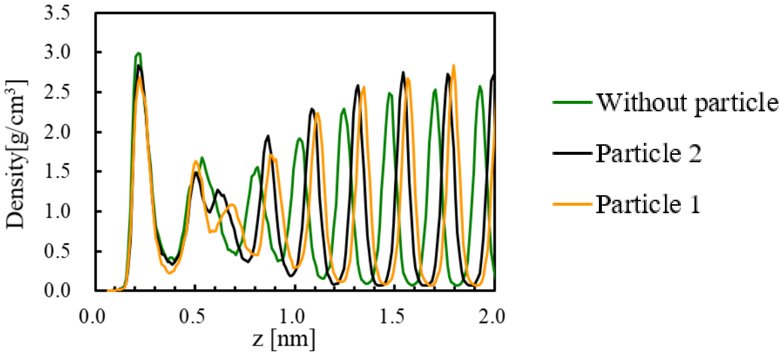

Figure 4. Density distribution of water molecules in the cases with and without particles in the vicinity of the wall surface.

Force acting on a Nanoparticle from the Solidification Interface

In order to clarify the influence of the ice interface on the particle, the forces acting on the particle were investigated. Figure 5 illustrates the time variation of the *z* direction force acting on the particle and the displacement of the particle's center of gravity (COM) in the perpendicular direction. In Fig. 5 (a) to Fig. 5 (c), the total force acting on the particles is donated as F_{total}, and the force acting from the water molecules and the wall surface are donated as F_{Water}, and F_{Wall}. Additionally, F_{z+} is the upward force acting on the particles, while F_{z-} is the downward force in the z axial direction.

After 25ns, the ice interface approaches the particle; the effect of the interface causes the particle to drift upwards. Such solidification interface and particle behavior is not typical in most cases, but some show similar dynamics. Focusing on the force and particle dynamics, Fig. 5 (a) reveals that F_{total} has not changed, even though the particles are moving. Conversely, the F_{water} and F_{wall} values are drastically changed and indicate a correlation between the z position of the particle and the force acting from the water molecules or wall on the particle in Fig. 5 (b) and Fig. 5 (c). This reveals that the ice interface affects the force acting on the particle.

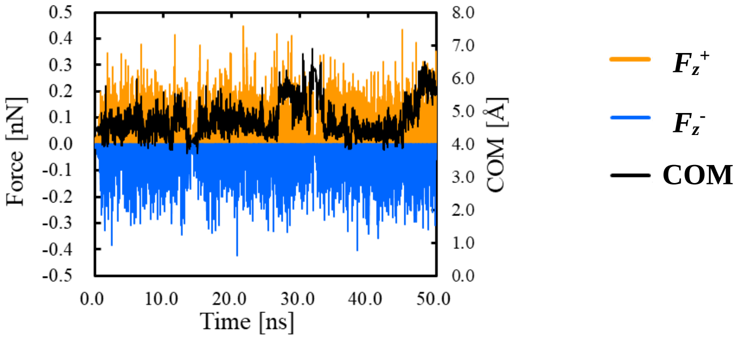

(a) F_{Total}

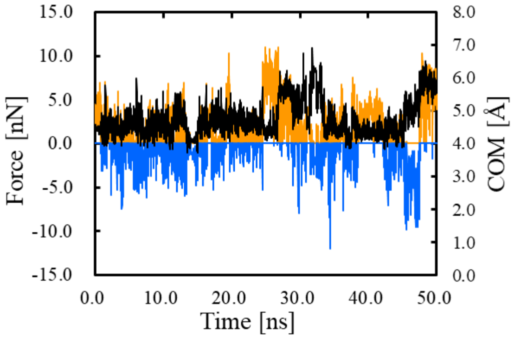

(b) F_{Water}

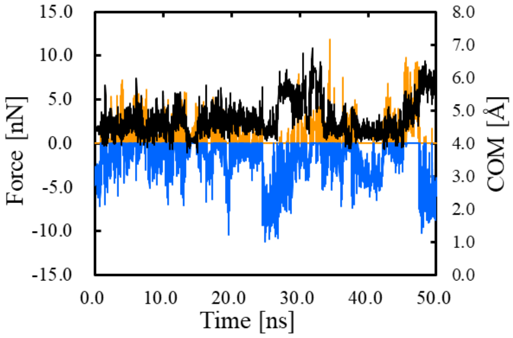

(c) F_{Wall}

Figure 5. Time evolution of force acting on a nanoparticle and center of mass of the nanoparticle.

Cooling Temperature and Force acting on a Nanoparticle

In order to clarify the influence of the cooling temperature on the solidification process, the cooling temperature conditions were changed to 241, 240, 238, and 236 K. Figure 6 reveals the time evolutions of the temperature and the total energy of the water molecules at each temperature increment. It indicates that the water temperature corresponded to the identified target temperature and the total energy curves decrease with time, indicating that the water is freezing. The total energy plateau at the start of the calculation (at the temperatures of 240K and 236K) implies that freezing has not progressed when the calculation started. Focusing on the total energy reduction rate that is shown by the dashed line in Figure 6 (b) at 236K and 240K, it indicates the solidification interface growth rate. In this calculation system, the total energy reduction rate increases as the cooling temperature decreases, and it implies that the lower cooling temperature, the faster the solidification interface growth rate.

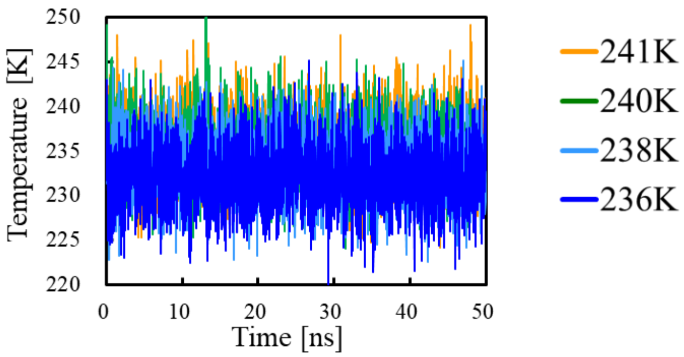

(a) Water temperature

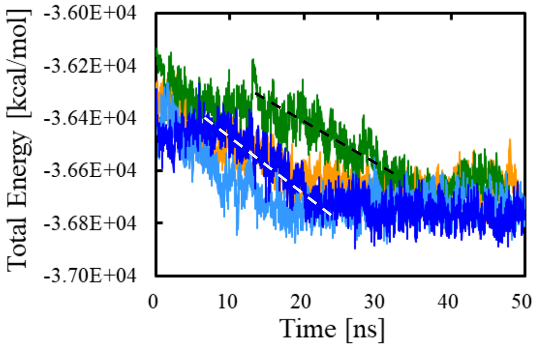

(b) Total energy of water molecules

Figure 6. Time evaluation of temperature and total energy of water molecules.

Figure 7 shows the *z* direction force that is acting on the particles from water molecules at each cooling temperature and the z direction displacement of the particles. The arrows in Fig. 7 indicate the time of contact between the solidification interface and the top of the particles. The solidification interface reaches to the wall surface temporarily and fluctuates on the wall's surface, and at each cooling temperature a quasi-liquid layer is continually evident between the surfaces of the ice and the wall.

Under all conditions, the solidification interface covered the particles and reached the vicinity of the wall surface. At the higher temperatures of 241 K and 240 K, F_{z+} shows that the direction of force acting on the particle is the opposite direction of the growth direction of the ice surface between *t* = 25-35 ns at 241 K and *t* = 13-15 ns at 240 K, as shown in Figs. 7 (a) and (b). Subsequently, the force direction acting on the particle is similar to the ice growth direction, which indicates that the direction of the force changes before and after contact between the solidification interface and the particle. However, under the lower temperature conditions of 238 K and 236 K, there is a slight force in the opposite direction to the ice surface growth; the force direction is largely the same as the growth direction of the ice surface shown in Figs. 7 (c) and (d). Regardless of the cooling temperature, after the solidification interface reaches the particles, it exerts a repulsive force.

Under high cooling temperature conditions of 241 K and 240 K, the attractive force acting from the solidification interface is related to the change in density profile of water due to solidification. This indicates that this attractive force becomes evident when the water density distribution changes slowly.

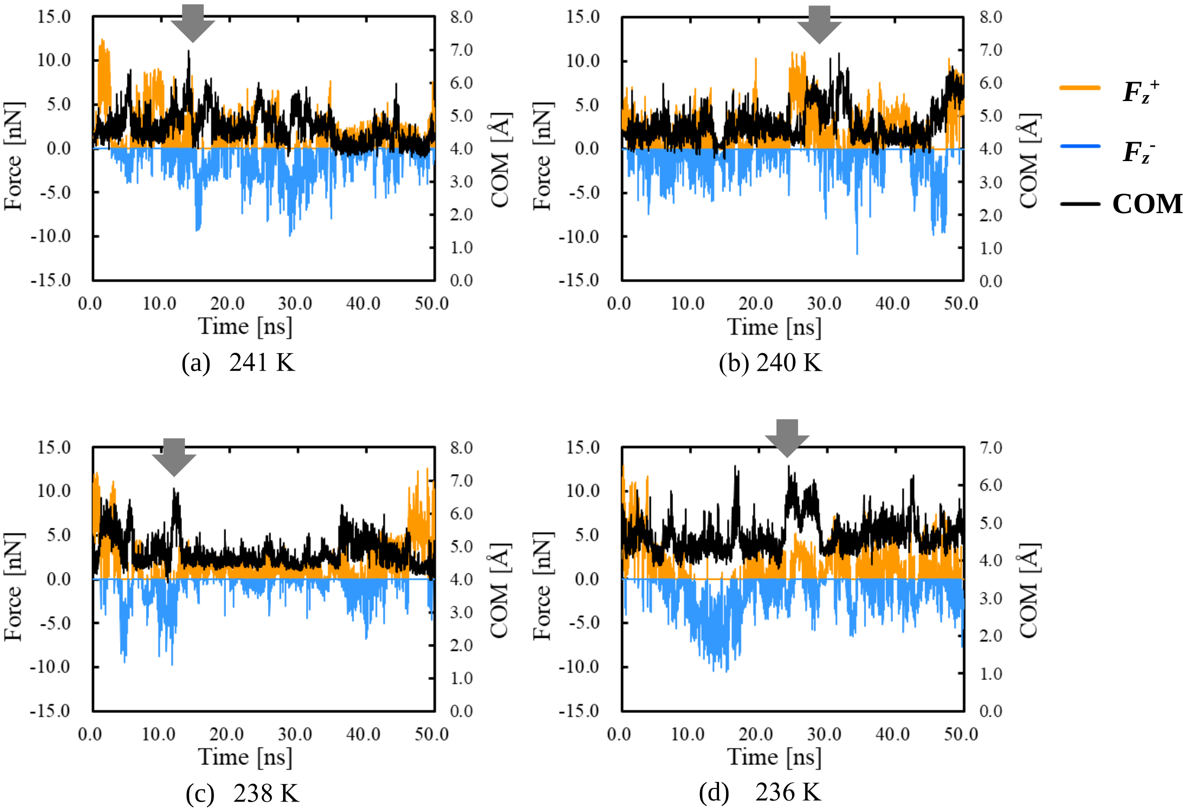

(a) 241 K

(b) 240 K

(c) 238 K

(d) 236 K

Figure 7. Time evolution of forces acting on nanoparticles from water molecules and center of mass of the nanoparticle at each temperature.

Conclusions

This study investigated the properties of water and ice on a solid surface with a nanoparticle in order to reveal the effects of water solidification on the nanoparticle in the vicinity of the solid surface. The results confirm that a strong mutual influence exists between the solidification interface and the nanoparticle on the wall's surface; the nanoparticle on the wall prevents water solidification in proximity to the wall. The force acting on the nanoparticle from water molecules changes as the solidification interface approaches; the cooling temperature is shown to affect the direction of this force. Under higher cooling temperature conditions, the growth of the solidification interface is slow. In this case, when the solidification surface approaches the nanoparticle, the direction of the force acting on the nanoparticle from the water molecule is opposite to the growth of the solidification surface; the force direction then aligns to that of the solidification interface. Conversely, under lower cooling temperature conditions, the solidification interface grows at a faster rate, and the force in the opposite direction of the solidification interface is smaller.

References

[1] J. An, H. Lee, H. Kim, and H. Jeong, “Effect of process parameters on particle removal efficiency in poly(vinyl alcohol) brush scrubber cleaning,” *Jpn. J. Appl. Phys.*, vol. 51, no. 2 PART 1, 2012. DOI: 10.1103/PhysRevB.31.5262

[2] K. Fujiwara and M. Shibahara, “A Molecular Dynamics Study on Wetting Phenomena at a Solid Surface with a Nanometer-Scale Slit Pore,” *Nano. Micro. Therm. Eng.*, vol. 17, no. 1, pp.1-9, 2008. DOI: 10.1080/15567265.2012.745636

[3] K. Miya, N. Fujiwara, M. Kato, and A. Izumi, “A New Cleaning Technology Using the Effect of Freezing Water on Wafer Surface,” *Electrochem. Soc.*, vol. 41, no. 5, pp. 215–220, 2011. DOI: 10.1149/1.3630846

[4] J. Jelassi, *et al.*, “Structural studies of water in hydrophilic and hydrophobic mesoporous silicas: An x-ray and neutron diffraction study at 297 K,” *J. Chem. Phys.*, vol. 134, no. 6, 2011. DOI: 10.1063/1.3530584

[5] K. Morishige and K. Nobuoka, “X-ray diffraction studies of freezing and melting of water confined in a mesoporous adsorbent (MCM-41),” *J. Chem. Phys.*, vol. 107, no. 17, pp. 6965–6969, 1997. DOI: 10.1063/1.474936

[6] D. Akporiaye, E. W. Hansen, R. Schmidt, and M. Stoecker, “Water-saturated mesoporous MCM-41 systems characterized by 1H NMR,” *J. Phys. Chem.*, vol. 98, no. 7, pp. 1926–1928, 1994. DOI: 10.1021/j100058a034

[7] E. W. Hansen, R. Schmidt, M. Stöcker, and D. Akporiaye, “Water-saturated mesoporous MCM-41 systems characterized by 1H NMR spin-lattice relaxation times,” *J. Phys. Chem.*, vol. 99, no. 12, pp. 4148–4154, 1995. DOI: 10.1021/j100012a040

[8] E. W. Hansen, M. Stöcker, and R. Schmidt, “Low-temperature phase transition of water confined in mesopores probed by NMR. Influence on pore size distribution,” *J. Phys. Chem.*, vol. 100, no. 6, pp. 2195–2200, 1996. DOI: 10.1021/jp951772y

[9] D. R. Uhlmann, B. Chalmers, and K. A. Jackson, “Interaction between particles and a solid-liquid interface,” *J. Appl. Phys.*, vol. 35, no. 10, pp. 2986–2993, 1964. DOI: 10.1063/1.1713142

[10] A. W. Neumann, J. Szekely, and E. J. Rabenda Jr., “Thermodynamic aspects of particle engulfment by solidifying melts,” *J. Colloid Interface Sci.*, vol. 43, no. 3, pp. 727–732, 1973. DOI: 10.1063/1.323217

[11] K. Tai, Y. Liu, and S. J. Dillon, “In situ cryogenic transmission electron microscopy for characterizing the evolution of solidifying water ice in colloidal systems,” *Microsc. Microanal.*, vol. 20, no. 2, pp. 330–337, 2014. DOI: 10.1017/S1431927613014128

[12] J. A. Hayward and A. D. J. Haymet, “Ice/water interface: molecular dynamics simulations of the basal, prism, $\{20\bar{2}1\}$, and $\{2\bar{1}\bar{1}0\}$ interfaces of ice Ih,” *J. Chem. Phys.*, vol. 114, no. 8, pp. 3713–3726, 2001. DOI: 10.1063/1.1333680

[13] H. Nada and Y. Furukawa, “Anisotropy in growth kinetics at interfaces between proton-disordered hexagonal ice and water: A molecular dynamics study using the six-site model of H2O,” *J. Cryst. Growth*, vol. 283, no. 1–2, pp. 242–256, 2005. DOI: 10.1016/j.jcrysgro.2005.05.057

[14] N. Giovambattista, P. J. Rossky, and P. G. Debenedetti, “Effect of Temperature on the Structure and Phase Behavior of Water Confined by Hydrophobic, Hydrophilic, and Heterogeneous Surfaces,” *J. Phys. Chem. B*, vol. 113, pp. 13723–13734, 2009. DOI: 10.1021/jp9018266

[15] Y. Naruke, S. Kosaka, T. Nakano, G. Kikugawa, and T. Ohara, “A molecular dynamics study on mass transport characteristics in the vicinity of SiO_2-water/IPA interfaces,” *Int. J. Heat Mass Transf.*, vol. 84, pp. 584–591, 2015. DOI: 10.1016/j.ijheatmasstransfer.2015.01.051

[16] S. M. Melnikov, A. Höltzel, A. Seidel-Morgenstern, and U. Tallarek, “Adsorption of water-acetonitrile mixtures to model silica surfaces,” *J. Phys. Chem. C*, vol. 117, no. 13, pp. 6620–6631, 2013. DOI: 10.1021/jp312501b

[17] A. Okuda, T. Nagasawa, S. Okawa, and A. Saito, “Research on Solidification of Water on Surface,” *14th Int. Conf. Prop. Water Steam Kyoto Water*, pp. 690–695.

[18] X. X. Zhang, M. Chen, and M. Fu, “Icing of water on polyethylene surfaces,” *Appl. Surf. Sci.*, vol. 313, pp. 771–776, 2014. DOI: 10.1016/j.apsusc.2014.06.070

[19] K. Fujiwara, S. Sasaki, and M. Shibahara, “A Molecular Dynamics Study on Effects of Solidification Phenomena on Water Molecules in the Vicinity of a Solid Surface,” *Therm. Sci. Eng.(in Japanese)*, vol. 25, no. 4, pp. 9–16, 2016. DOI: 10.11368/tse.25.9

[20] T. Schneider and E. Stoll, “Molecular-dynamics study of a three-dimensional one-component model for distortive phase transitions,” *Phys. Rev. B,* vol. 17, no. 3, pp. 1302–1322, 1978. DOI: 10.1103/PhysRevB.17.1302

[21] J. L. F. Abascal and C. Vega, “A general purpose model for the condensed phases of water: TIP4P/2005,” *J. Chem. Phys.*, vol. 123, no. 23, 2005. DOI: 10.1063/1.2121687

[22] F. H. Stillinger and T. A. Weber, “Computer simulation of local order in condensed phases of silicon,” *Phys. Rev. B,* vol. 31, no. 8, pp. 5262–5271, 1985. DOI: 10.1016/j.colsurfa.2004.04.005

[23] S. Plimpton, “Fast Parallel Algorithms for Short-Range Molecular Dynamics,” *J. Comput. Phys.*, vol. 117, no. 1, pp. 1–19, 1995. DOI: 10.1006/jcph.1995.1039

[24] K. Koga, H. Tanaka, and X. C. Zeng, “First-order transition in confined water between high-density liquid and low-density amorphous phases,” *Nature,* vol. 408, no. 6812, pp. 564–567, 2000. DOI: 10.1006/jcph.1995.1039

[25] R. García Fernández, J. L. F. Abascal, and C. Vega, “The melting point of ice Ih for common water models calculated from direct coexistence of the solid-liquid interface,” *J. Chem. Phys.*, vol. 124, no. 14, pp. 1–11, 2006. DOI: 10.1063/1.2183308

[26] S. Engemann, *et al.*, “Interfacial Melting of Ice in Contact with SiO_2,” *Phys. Rev. Lett.*, vol. 92, no. 20, p. 205701, 2004. DOI: 10.1103/PhysRevLett.92.205701